Biomaterials Science

ROYAL SOCIETY OF CHEMISTRY

PAPER

View Article Online
View Journal | View Issue

Cite this: *Biomater. Sci.*, 2022, **10**, 2609

Escherichia coli response to subinhibitory concentrations of colistin: insights from a study of membrane dynamics and morphology†

Ilanila Ilangumaran Ponmalar, ‡[a] Jitendriya Swain ‡[b] and Jaydeep K. Basu *[b]

Prevalence of widespread bacterial infections brings forth a critical need to understand the molecular mechanisms of the antibiotics as well as the bacterial response to those antibiotics. Improper use of antibiotics, which can be in sub-lethal concentrations is one among the multiple reasons for acquiring antibiotic resistance which makes it vital to understand the bacterial response towards sub-lethal concentrations of antibiotics. In this work, we have used colistin, a well-known membrane active antibiotic used to treat severe bacterial infections and explored the impact of its sub-minimum inhibitory concentration (MIC) on the lipid membrane dynamics and morphological changes of *E. coli*. Upon investigation of live cell membrane properties such as lipid dynamics using fluorescence correlation spectroscopy, we observed that colistin disrupts the lipid membrane at sub-MIC by altering the lipid diffusivity. Interestingly, filamentation-like cell elongation was observed upon colistin treatment which led to further exploration of surface morphology with the help of atomic force spectroscopy. The changes in the surface roughness upon colistin treatment provides additional insight on the colistin–membrane interaction corroborating with the altered lipid diffusion. Although altered lipid dynamics could be attributed to an outcome of lipid rearrangement due to direct disruption by antibiotic molecules on the membrane or an indirect consequence of disruptions in lipid biosynthetic pathways, we were able to ascertain that altered bacterial membrane dynamics is due to direct disruptions. Our results provide a broad overview on the consequence of the cyclic polypeptide colistin on membrane-specific lipid dynamics and morphology of a live Gram-negative bacterial cell.

Received 9th January 2022,
Accepted 26th March 2022

DOI: 10.1039/d2bm00037g

rsc.li/biomaterials-science

1 Introduction

Traditionally, antibiotics are widely used to treat a broad spectrum of prevalent bacterial infections.[1] Common modes of action of classical antibiotics include targeting the bacterial outer membrane, peptidoglycan and the inner membrane and its synthesis machinery.[2] Additional modes of action include targeting DNA replication which in turn disrupts bacterial fission and growth, and disrupting specific protein synthesis pathways by suppressing or overexpressing proteins central to the signaling pathways.[3] Among the abovementioned mechanisms, targeting the bacterial cell envelope is strategically effective and provides specificity against pathogens due to the unique structure and composition of bacterial cell wall.[4] Therefore, understanding the interaction of such membrane targeting antibacterial molecules with the bacterial cell envelope at the molecular level should give us additional insight into antimicrobial action. These studies will enable the development of drug molecules to combat bacterial infections and suppress the emergence of drug-resistant strains.[5]

Although *Escherichia coli* is a conventional facultative anaerobe that is observed in abundance as a part of the gut microbiome, virulent strains are known to cause various infections such as bloody diarrhea and gastroenteritis.[6] In addition to the diarrheal diseases, the pathogenic *E. coli* also causes meningitis and urinary tract infections.[7] Enterohemorrhagic *E. coli* are seen in undercooked poultry and meat products.[8] Antibiotics are extensively used in treating multiple bacterial infections in the poultry[9] and meat industries.[10] Uncontrolled use of antibiotics has led to the development of resistant bacterial strains that has necessitated the discovery of a new generation of antibiotics.[11] Methicillin-resistant *Staphylococcus aureus* (MRSA) and multidrug-resistant tuberculosis (MDR-TB) are prevalent and challenging to treat with multiple

[a]*Center for BioSystems Science and Engineering, Indian Institute of Science, Bengaluru 560012, India*
[b]*Department of Physics, Indian Institute of Science, Bengaluru 560012, India. E-mail: basu@iisc.ac.in; Tel: +91 080 2293 3281*

†Electronic supplementary information (ESI) available. See DOI: https://doi.org/10.1039/d2bm00037g

‡Contributed equally to the work.

antibiotics.[12,13] In order to combat these emerging multidrug-resistant strains, colistin, has been rediscovered as a potential drug to be used in combination with other antibiotics.[14]

Among many antibiotics, colistin (polymyxin E) is a well-known membrane-active drug which is an amphiphilic positively charged cyclic polypeptide.[15] They target the negatively charged lipopolysaccharide (LPS) and replace the Ca^{2+} or Mg^{2+} ions in the core oligosaccharide region. One longstanding hypothesis is that colistin molecules disrupt the physical integrity of the bacterial cell membrane, causing leakage of intracellular contents.[16] Several recent studies have explored how colistin interacts with the bacterial cell model membranes using transmission electron microscopy (TEM) and other techniques. Membrane permeability due to the action of colistin on small unilamellar vesicles and erythrocytes were shown using calcein leakage and hemolysis assays.[17–19] Additionally, when colistin attacks the membrane, lipid remodelling occurs and is reported to form nanoclusters (~2 nm) as well as macroclusters that protrude from the bilayer.[17] This was confirmed with atomic force microscopy studies. Insights into the binding and penetration of colistin into lipid membrane are investigated using lipid monolayers at the air–water interface.[18,20,21] In contrast to the abundant studies of colistin interacting with LPS in vesicular or monolayer systems, only a few reports of colistin–LPS interactions in a planar bilayer setup have been made.

Due to the complex structure of the bacterial cell envelope, constructing realistic bacterial membrane models to carry out *in vitro* studies is an active area of research.[22] The lipids present on the inner as well as outer membranes of the bacterial cell envelope undergo different types of diffusion that includes lateral diffusion, flip-flops, and inter-membrane lipid transfers. Although lipid and protein diffusion on mammalian cell membranes have been discussed in multiple reports, recent experiments have revealed unique protein dynamics on the bacterial cell membrane[23–25] which typically occurs on a longer time scale compared to lipid lateral diffusion. However, it is challenging to carry out diffusion measurements using techniques such as fluorescence correlation spectroscopy (FCS) on live bacterial cell membrane due to its small size.[26] Measuring the lipid lateral diffusion on model membranes[27,28] is comparatively simpler for understanding the mechanism of membrane interaction with external molecules. Our group has worked extensively on measuring lipid lateral diffusion on model membrane systems to elucidate the action of membrane-active molecules such as anti-microbial peptides, pore-forming toxins,[29–31] and nanoparticles[32,33] on the lipid bilayer. While the *z*-dependent lipid diffusion could be addressed with membrane-specific labels, lipid lateral diffusion provides information on standard membrane properties such as lipid packing, disorder, lipid composition and are typically correlated with membrane permeability, depolarization, micro- and nano-domain formation/coalescence. The lipid dynamics has revealed significant information about microscopic changes in membrane organization which can correlate with altered cell functionality and signaling and hence is a very crucial probe especially for bacterial cellular response to antibiotics. However, to the best of our knowledge, lipid diffusion on live bacterial cell membranes has been rarely reported to date.[25]

It is important to note that the colistin concentrations at which bacterial cell lysis is observed are much less in comparison with the reported values used in the model lipid membrane.[17,18] Antibiotics such as colistin are effective only when the concentrations used are higher than the minimum inhibitory concentration (MIC) between consecutive doses prescribed. When the pathogens are treated with sub-MIC antibiotic doses, they tend to evolve resistance against that particular antibiotic through various mechanisms.[34] Sub-minimum inhibitory concentrations of colistin promote the formation of biofilm in *Acinetobacter baumannii* which makes it more tolerant towards antibiotics.[35] Laboratory evolution of colistin resistance using sub-MIC of colistin resulted in genetic mutations that helped in retaining the virulent properties of *Acinetobacter baumannii*.[36] The consequences of sub-MIC colistin exposure on pathogens continuously for generations resulted in providing opportunity for the pathogens to survive in lethal doses. Hence, the main objective of our work is to understand the biophysical as well as morphological changes and response of lipids present in the live cell membrane of the Gram-negative bacterial cell wall towards the accumulation of sub-inhibitory concentration of colistin.

For this study, we have used wild type *E. coli* K12 treated with sub-MIC colistin to understand the biophysical and morphological changes on the cell envelope that occur as a consequence of colistin action. Here, we have successfully applied fluorescence correlation spectroscopy and atomic force microscopy (AFM) techniques to demonstrate that colistin causes significant changes to the morphology and lipid diffusivity on the *E. coli* K12 cell membrane at sub-MIC. Our study has direct implications on identifying how exposure to sub-MIC concentrations of colistin might help in membrane-based modifications that could potentially prevent cell lysis. It is imperative to suggest that enhanced lipid dynamics due to membrane reorganization at sub-MIC is not lethal but modifies the bacterial membrane due to direct physical interaction.

2 Experimental methods

2.1 Materials

E. coli NCTC 13846 was procured from Public Health England (PHE) cell cultures in the form of lyophilized pellet which was then reconstituted in the growth media and glycerol stock was prepared for storage purpose. Nutrient media Luria–Bertani (LB), agar, colistin sulfate, hydrogen peroxide, and Nile red were procured from Merck-Sigma Aldrich (USA). FM4-64 was procured from Thermo Fisher Scientific (USA).

2.2 *E. coli* growth kinetics

Glycerol stock of *E. coli* K12 was reconstituted in Luria–Bertani (LB) broth and plated in LB agar. The plate was incubated at 37 °C overnight and stored at 4 °C for further culturing.

Primary culture is prepared by incubating a single colony of cells in 5 ml LB and grown overnight at 37 °C with continuous shaking. 1% inoculum was used for growing the cells which are subsequently taken for imaging and FCS experiments. For the growth studies, cells from the primary culture were inoculated in 2 ml LB with and without antibiotics (or) H_2O_2 in a 24-well plate. The plate was then kept inside a Tecan Plate reader with continuous shaking at 37 °C. Turbidity readings were taken at OD_{620nm} for every 15 min up to a total duration of 5 hours and the data is fitted to obtain specific growth rates.

2.3 *E. coli* membrane labeling and length determination

All the experiments on bacterial membranes were carried out when the cells are within the log phase with the OD of ~0.2 to 0.4. *E. coli* K12 cells that were grown for 2 hours in 5 ml LB at 37 °C were labeled with Nile red, rinsed and then fixed to a poly-L-Lysine (PLL) coated glass coverslips. Depending on the experiment, LB media is added with appropriate concentration of antibiotics or H_2O_2. PLL helps in fixing the bacteria to the coverslip so that the cells do not move during imaging. 2–5 μl of the re-suspended cells are added to the coverslips and gently spread using a sterile tip. The cells are rinsed with PBS to remove free unbound cells. PBS is then added to the coverslip and during the entire experiment, the cells are immersed in PBS. Images were procured using a SP5-Leica confocal laser scanning microscope (Leica Microsystems, Germany). The length of the bacteria is measured by drawing a line profile along the entirety of the cell and the length measured from multiple bacteria is illustrated in the form of histograms.

2.4 Fluorescence correlation spectroscopic (FCS) measurements

For all dynamics related experiments, the FCS measurements were carried out on the polar region of the cells and the resulting histograms are the compilation of data from 5–6 different bacteria with approximately 10–20 readings per bacterium. All experiments were performed in triplicate and the mean data are expressed as the mean ± standard deviation unless otherwise mentioned. Photon intensities were collected using the avalanche photo diode (APD) detector 581–654 nm filter for Nile red and 647–703 nm for FM4–64. The intensity was correlated using the PicoQuant Symphotime software. The correlation curves were analyzed and fitted using a standard 2D auto-correlation equation. The diffusion coefficient was evaluated using,

$$D = \frac{\omega^2}{8\tau_D \ln 2} \quad (1)$$

where ω is the full width half maximum (FWHM) of the confocal beam.[28]

2.5 Atomic force microscopic (AFM) imaging

The bacterial cells are immobilized on the glass coverslips using PLL. The coverslip is placed on the sample holder of AFM stage (Park Systems, South Korea) and the imaging is carried out using tapping non-contact mode in air. Imaging of cells were always performed at room temperature (T = 23 °C). The images were taken in using PNP-TR2 (NanoWorld, Switzerland) AFM probe with a set point of 0.2 nN force.

3 Results and discussion

3.1 Role of sub-inhibitory concentration colistin on lipid membrane dynamics of *E. coli*

All the following experiments on bacterial membranes were carried out after 2 h of incubation when the cells are within the log phase with the OD of ~0.2 (ESI Fig. SF1†). Nile red, lipid-specific hydrophobic dye, was used for the imaging of the live bacterial membrane (Fig. 1A and B). Fig. 1A and B images reveal that Nile red is localized along the membrane of bacteria. The control *E. coli* K12 cells are revealed to be rod-shaped with an average length 2.01 ± 0.51 μm long (Fig. 1C), which is typical of a standard *E. coli*.[37] The mean values are reported with their corresponding standard deviation across three sets of experiments unless otherwise mentioned. Lateral diffusion of Nile red molecules along the lipid bilayer was measured using FCS (see Methods) and is observed as a representative of the lipid lateral diffusion. Molecular dynamics simulation studies on lipid bilayer with Nile red have revealed that the dye prefers to be positioned near the head group of the lipid bilayer.[38] The histogram for the Nile red diffusion coefficients measured on the wild-type *E. coli* cell membrane is shown in Fig. 1D. The average Nile red diffusion is 1.43 ± 0.36 $\mu m^2\ s^{-1}$. The anomaly parameter, which defines the deviation from free Brownian diffusion, α was also fitted and found to be 0.85 ± 0.13 as shown in Fig. 1E. The data reveals that the lipid diffusion in bacterial membranes is lower when compared to the model cell membranes where lipid diffusivities on giant unilamellar vesicles ranged from 6–12 $\mu m^2\ s^{-1}$ (ref. 22, 39 and 40) and supported lipid bilayers ranged from 1–6 $\mu m^2\ s^{-1}$.[33,41,42] Such lowered diffusion coefficients are expected in the live bacterial cell membrane and mammalian cell membranes[43] which are generally attributed to the complex crowded environment of the cell membrane enriched with various transmembrane proteins. The anomaly parameter, α, which is a measure of the deviation from Brownian diffusion also suggests that the presence of membrane proteins in this purportedly crowded environment affects the Nile red diffusion. In order to understand the effects of the membrane disrupting antibiotic, colistin, Nile red diffusion in wild-type *E. coli* is assumed as the control. Thus, any changes in the Nile red diffusion observed in the membrane were solely a consequence of the antibiotic.

Initial experiments are carried out to measure the MIC of colistin on *E. coli* and its corresponding growth kinetics. For all sub-MIC experiments, 0.5 $\mu g\ ml^{-1}$ concentration of colistin was used which corresponds to 0.25 MIC. We have observed that cells incubated with sub-inhibitory concentration of colistin (0.25 MIC) showed significantly reduced growth rates with

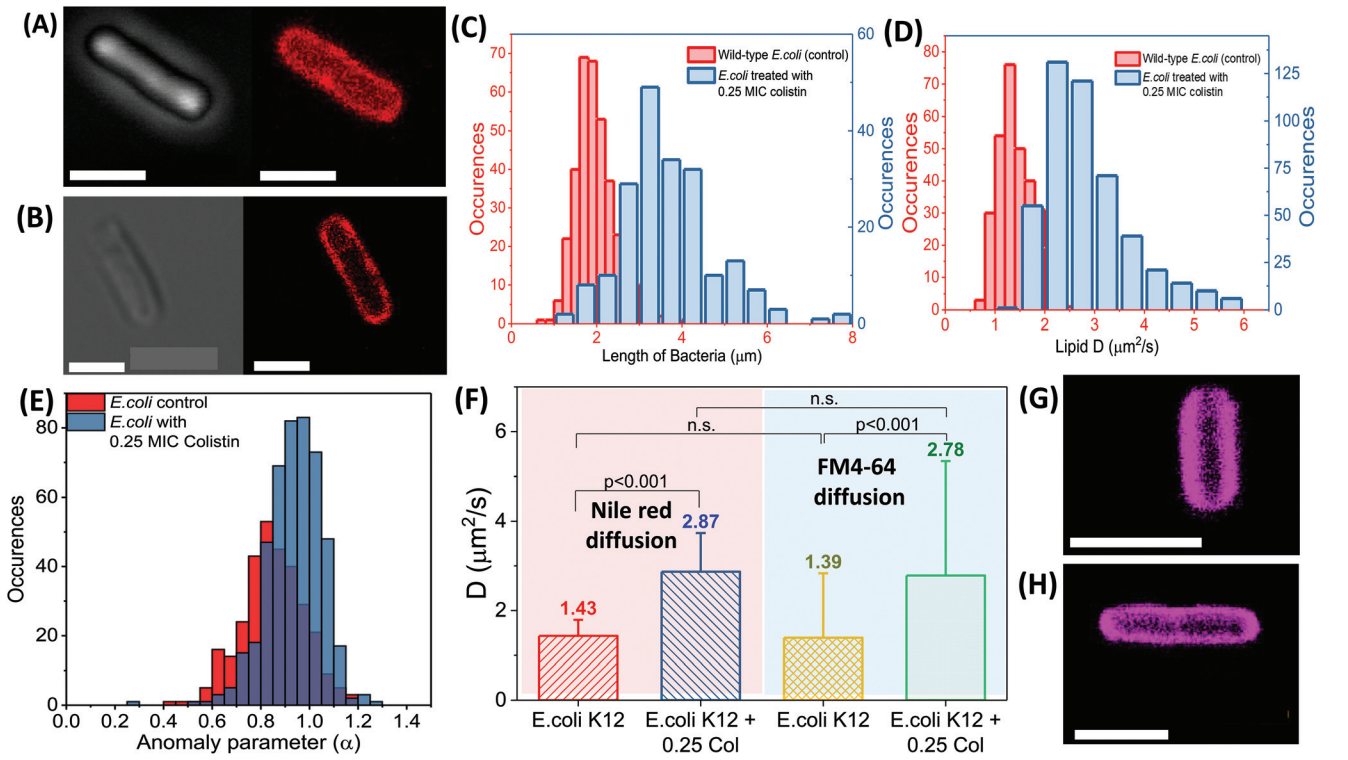

Fig. 1 (A) Phase contrast and confocal images of a typical Nile red labelled *E. coli* wild-type cell. Corresponding images taken for the cells treated with 0.25 MIC colistin is provided in the panel (B). (C) Size distribution of the bacterial cells with and without colistin treatment. (D) Histogram of Nile red diffusion coefficients in bacterial cells. (E) Histogram of anomaly parameter (α) in bacterial cells. (F) Average diffusion coefficients measured for Nile red (red) and FM4-64 (blue) labelled cells with and without colistin treatment. (G) Confocal image of *E. coli* labelled with FM4-64 and its corresponding colistin treated bacteria is provided in the panel (H). Color code for panels (C, D and E) – Red bars: Without colistin; Blue bars: With colistin. Scale bar is 2 μm. All experiments are performed in triplicates, $30 < n < 50$ cells.

a longer lag phase (ESI Fig. SF1†). These results are in good agreement with the earlier reports.[44] After 2 h of growth in the presence of 0.25 MIC colistin, the physical attributes such as length of the cells were different from that of the control as shown in Fig. 1C. The cells have elongated in size with an average length of 3.68 ± 1.12 μm (Fig. 1C). We also observed that a very small population of bacteria had bleb-like structures on them (see the ESI Fig. SF4†). When the Nile red diffusion was measured, we have also observed that the diffusion coefficients had increased when cells were grown in the presence of 0.25 MIC colistin for 2 h. It is to be noted that the Nile red diffusivity is independent of different lengths of bacteria treated with colistin (Fig. 2). The average D value was 2.87 ± 0.87 $\mu m^2\ s^{-1}$, which is 2 times greater than that of the control (Fig. 1D and F). Comparing the diffusion coefficients measured on the wild-type and antibiotic treated *E. coli* cells as given in Fig. 1C and F, we can see that there is significant increase observed in the colistin treated cells.

In contrast to the increase in lipid diffusivities observed on live bacterial cell membranes, recent measurements on model supported lipid bilayers show a decrease in diffusivities when treated with colistin[45] due to the binding of colistin on the membranes. The supported lipid bilayers used in these experiments are constituted with phosphatidyl ethanolamine (PE), phosphatidyl glycerol (PG) and cardiolipin (CL) lipids to mimic the inner membranes of Gram-positive and Gram-negative bacterial cell walls. Further, it is interesting to note that their samples were devoid of LPS which are the primary binding sites for colistin.[45] Comparing the results obtained from model membrane systems to the live cells, we can emphasize on the fact that the negatively charged primary binding site of colistin, LPS plays a significant role in the membrane disruption by altering the lipid packing. The electrostatic interactions happening between LPS and colistin could be the one of the underlying reasons behind the observed membrane modifications. Interestingly, another report on molecular dynamics simulation have shown that the antibiotic, polymyxin B, which is in the same class of molecules as colistin, is reported to loosen the LPS containing outer membrane and stiffen the inner membrane[46] which proves that LPS interaction with colistin is significant. Enhanced lipid dynamics and increase in area per lipid are generally observed when an external molecule such as thymol enters the lipid bilayer.[22] Correlating the changes observed in the lipid dynamics of LPS containing membranes, we can postulate that colistin can bind to all lipid membranes but enters and loosens the membrane only in the presence of LPS.

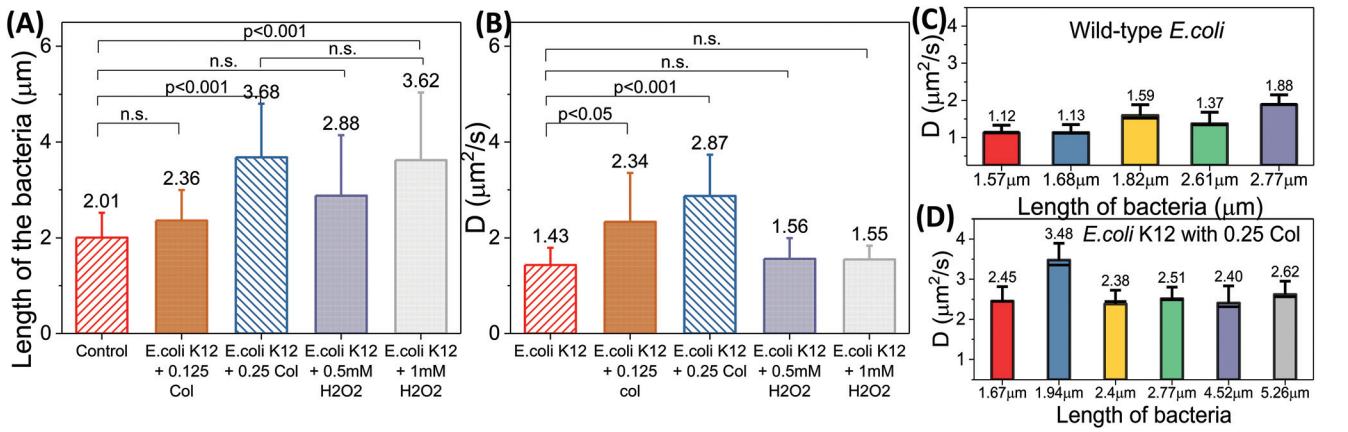

Fig. 2 Comparison of average bacterial length (A) and Nile red diffusion coefficients (B) for wild-type *E. coli* with colistin and hydrogen peroxide treated cells. Color code: Red – Wild-type *E. coli*; Brown – 0.125 MIC colistin treated cells; Blue – 0.25 MIC colistin treated cells; Purple – 0.5 mM H_2O_2 treated cells; Grey – 1 mM H_2O_2 treated cells. Average Nile red diffusion coefficients of single wild-type *E. coli* (C) and colistin treated *E. coli* (D) across different cell lengths. All experiments are performed in triplicates, $30 < n < 50$ cells.

Focusing on mean values of the anomaly parameters α extracted from these membrane dynamics for the antibiotic treated cells (Fig. 1E), the values did not significantly differ from the wildtype cells demonstrating the anomalous behavior of the lipid dynamics observed even during the colistin interaction. Although it is well known from the plasma membrane literature that an increase in lipid diffusivity can be attributed to either disordering of the membrane?[47] or an increase in lipid free area?[48] measurements of lipid dynamics in bacterial membranes exposed to antibiotics are lacking in the literature. Hence, some of the potential possibilities that can cause such enhanced diffusion coefficients include changes in the Nile red itself due to the action of colistin, the physical elongation of the cell, or changes in the lipid membrane due to direct interaction of the colistin molecule on the membrane. Additionally, in the case of live bacterial cells, one of the important factors that can potentially contribute to changes in Nile red diffusion are variations in membrane composition that are observed when *E. coli* adapts to acquire antibiotic resistance.[49] In the following sections, we have systematically verified the above-mentioned possibilities using different methodologies to identify the exact reason behind enhanced lipid fluidity due to colistin interaction at sub-MIC levels.

Further to prove that our above mentioned observation is independent of the lipid dye used for the measurements, we have used another well-known lipophilic styryl dye, FM4–64 (*N*-(3-Triethylammoniumpropyl)-4-(6-(4-(Diethylamino) Phenyl) Hexatrienyl) Pyridinium Dibromide) that has been used widely for imaging cell membranes.[50] From Fig. 1G and H, we have observed that the FM4–64 dye was spread homogeneously on the *E. coli* cell envelope although its specificity in binding to the particular component of the cell envelope is not reported,[50] it is known to prefer labelling the bacterial inner membrane.[51] When FCS was carried out on the FM4–64 labelled wild-type cells that are treated and untreated with colistin, the diffusion values measured were similar to the Nile red diffusion as shown in Fig. 1F. The FM4–64 diffusion coefficient of the wild-type cells are observed to be 1.39 ± 1.04 and for colistin treated cells, it is reported to be 2.78 ± 1.55. This gives us additional evidence that the Nile red diffusion coefficients are indeed representative values of lipid diffusion on the cell membrane.

3.2 Lipid dynamics do not depend on cell elongation and lipid composition

In order to correlate the elongation caused due to antibiotic stress on bacteria with lipid diffusion, we carried out experiments by incubating the cells with hydrogen peroxide to induce oxidative stress. It has been reported earlier that the oxidative stress induced by H_2O_2 affects the cell morphology and protein synthesis.[52] Hence, we incubated the cells with 0.5 and 1 mM H_2O_2 for a period of two hours and repeated the imaging, FCS and growth experiments. Size analysis on the H_2O_2-treated cells showed that it does affect the cell morphology and the average length of the bacteria is found to be 3.62 ± 1.42 μm for (1 mM H_2O_2) which is significantly larger compared to the control cells and is similar to the colistin-treated cells. Concentration-dependent size distribution is shown in Fig. 2A. These sizes are comparable to that of the colistin-treated cells. When Nile red-labeled cells were observed under confocal beam for FCS, the average lipid diffusivity was 1.55 ± 0.29 $\mu m^2\ s^{-1}$ with an average α values of 0.90 ± 0.14. The Nile red diffusion values shown in Fig. 2B shows that the diffusivity of lipids was not enhanced as observed in the colistin treated cells. This particular experiment was carried out for 0.5 mM H_2O_2 and the lipid diffusivities were not significantly different when compared with Nile red diffusion measured on the control cells.

Apart from 0.25 MIC colistin, 0.125 MIC colistin-treated cells are investigated for obtaining size distribution and lipid diffusion. Interestingly at log phase, the cells treated with 0.125 MIC colistin were 2.36 ± 0.63 μm long which was not sig-

nificantly different from the control cells. Surprisingly, we observed changes in the Nile red diffusion. The mean D value is observed to be 2.29 ± 0.94 with the anomaly parameter α of 0.839 ± 0.09. Correlating the changes observed with respect to altered D values observed from 0.125 MIC treated cells to the un-altered D values observed from 1 mM H_2O_2, we can confirm that the bacterial membrane dynamics independent of the modified cell length due to filamentation/elongation. This data also signifies that values of the bacterial length as well as lipid D depend on the concentration of colistin used.

Additionally, to validate our earlier claim that the cell growth rates do not affect lipid diffusivities, the growth curves were evaluated for the cells incubated with 0.5 and 1 mM H_2O_2 based on the time-dependent turbidity values measured at 620 nm. As provided in ESI Fig. SF1,† growth rates decreased for cells under oxidative stress and the lag time increased with increasing concentration of H_2O_2. This retarded growth was similar to trends observed with colistin treated cells (ESI Fig. SF1†) where we found that the lipid diffusivities were significantly enhanced from the control experiments (Table ST1†). Similarly, when compared with the control cells where the cells were grown in the absence of stress, the growth rates for cells treated with H_2O_2 were distinctly slower. However, despite these slower growth rates, the lipid diffusivities were similar to the control cells (ESI Table ST1†) and independent of the concentration of H_2O_2. The extent of elongation with the H_2O_2 treated cells were also similar to the elongation observed with the colistin treatments (ESI Table ST1†), providing additional confirmation to the lack of correlation between increased lipid diffusion and cell elongation. Taken together, the results observed on cells treated with H_2O_2 and cells treated with colistin provide strong evidence for the following. The increase in lipid diffusion depends on the nature of the stress (oxidative or antibiotic) and does not depend on the cell growth kinetics or the extent of elongation. These results suggest that the observed changes in lipid diffusion arise from a modulation in the membrane lipid composition at sub-inhibitory levels of antibiotics.

We have further extended our lipid dynamics experiments in another strain of *E. coli*, which has a gene that introduces modifications on the outer leaflet of the cell envelope by introducing the phosphatidylethanolamine groups. This strain NCTC 13846 (National Collection of Type Cultures) has a plasmid that encodes mcr-1 (mobilized colistin resistance-1) gene that has been reported to modify the charge on the membrane by introducing phosphatidylethanolamine residue (pEtN) on the head group of lipid A thereby neutralizing the negative charge of LPS.[49] We wanted to explore the relationship between the enhanced lipid diffusion observed at sub-MIC of colistin to a different strain of *E. coli* to check if there is any change in lipid composition of the cell envelope that is causing the lipid disorderness and surface roughness. The *E. coli* NCTC 13846 strain was grown in the presence of 10 μg ml^{-1} of colistin (Fig. 3A). Although the lipid compositions of the mutant strain are modified in comparison to the wild-type *E. coli*, interestingly, we could observe that these strains are similar to wild-type *E. coli* cells in the absence of colistin and are significantly different from the colistin-treated wild-type cells. The *E. coli* NCTC 13846 strain grown in the presence of colistin was 2.03 ± 0.36 μm in length (Fig. 3B) with the mean Nile red diffusion coefficient of 1.63 ± 0.81 $\mu m^2\ s^{-1}$ (Fig. 3C) which is significantly different from the colistin treated wild-type *E. coli* cells indicating that lipid modifications are not related to the changes in the membrane fluidity and incubation of cells with sub-MIC colistin does not cause lipid alterations similar to mcr-1 gene based lipid modifications. The results from our work are in good agreement with the recently reported works, where membrane permeability was measured as a function of concentration and compared them with the mcr-1 plasmid containing *E. coli*.[53,54] The membrane permeability was measured using the propidium iodide dye on bulk solution.[55] Similar to the diffusion values, the permeability of the mutant strains did not vary significantly while the colistin treated susceptible cells became permeable with time. Hence, membrane permeability induced lipid disorderness might be one of the causes behind the enhanced lipid diffusion. To validate the colistin–membrane interactions hap-

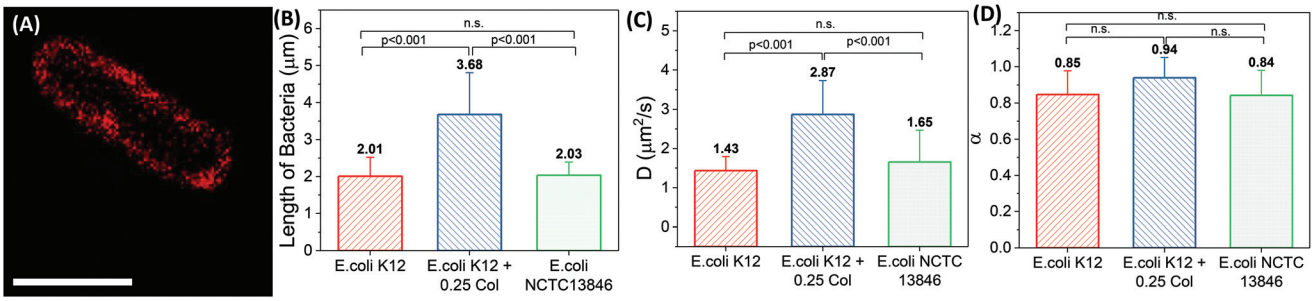

Fig. 3 (A) Confocal fluorescent image of a sample *E. coli* NCTC 13846 cell labelled with Nile red. Comparison of wild-type *E. coli* average cell length (B), Nile red diffusion coefficients (C), and anomaly parameter α (D) with 0.25 MIC colistin treated cells and *E. coli* NCTC 13846 grown in 10 μg ml^{-1} colistin. Scale bar is 2 μm. All experiments are performed in triplicates, $30 < n < 50$ cells.

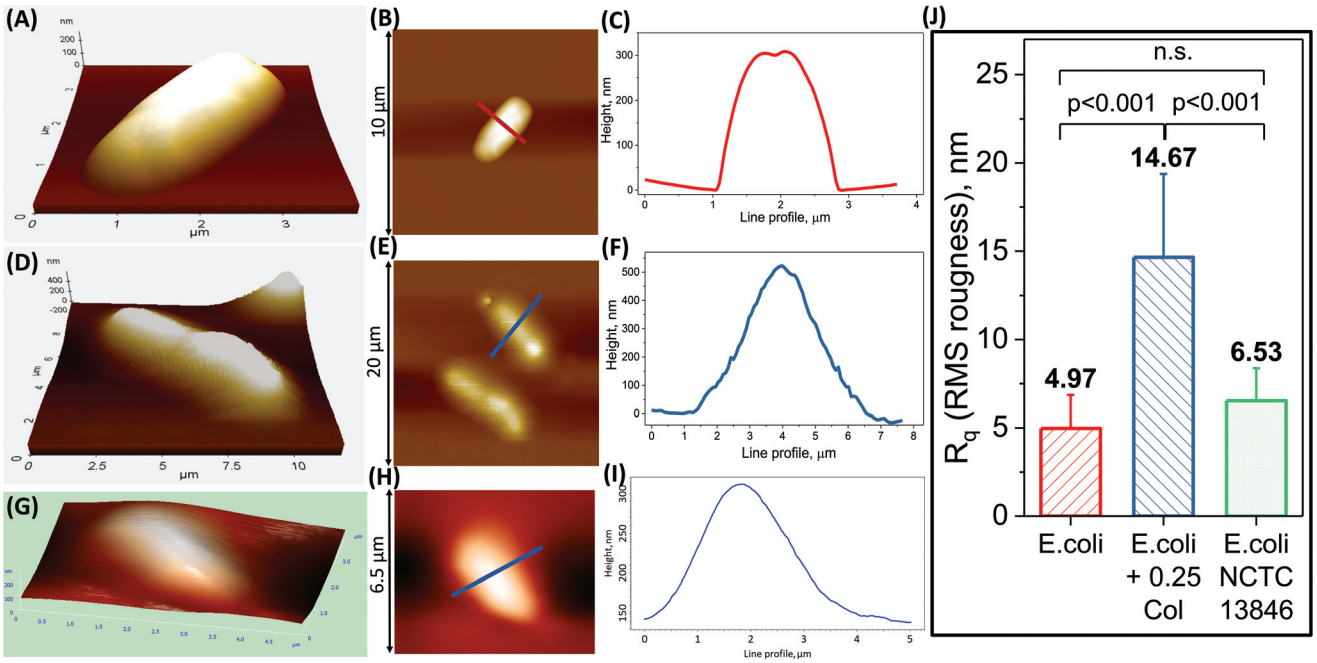

Fig. 4 Atomic force microscopic image of wild-type *E. coli* in 3-dimension (A) and 2-dimension (B) taken in air and corresponding line profile across the cell is plotted in panel (C). Similar images and line profiles are plotted for wild-type *E. coli* treated with 0.25 MIC colistin (D and E) and (F) and *E. coli* NCTC 13846 strain (G and H) and (I). (J) Mean surface roughness measured across different cells. All experiments are performed in triplicates, $15 < n < 20$ cells.

pening on the surface of the cells, AFM was carried out to measure surface properties.

3.3 Role of sub-inhibitory concentration of colistin on surface morphology of the *E. coli* cells

The surface morphology of the cells is studied using the standard atomic force microscopic imaging in air. The control cells as well as colistin treated cells are imaged in air using non-contact mode which is typically carried out for imaging bacterial cells.[56] The wild-type bacterial cells were imaged after ~5–10 min exposure to air for all the samples to avoid imaging artifacts due to drying (Fig. 4A–C). While imaging in air, we could observe that upon treatment with colistin, the physical attributes of the *E. coli* such as the cell width and the cell height were ~4 μm and ~500 nm (Fig. 4D–F). In comparison to the wild-type cells that are ~2 μm wide and ~300 nm high, the colistin treated cells are larger in physical morphology. Although, we did not observe such variation in width while imaging in confocal fluorescence microscope due to resolution limitation, one of the reasons that can attribute to such changes is that the cells are imaged in air during AFM. Such morphological differences between air-imaging and liquid imaging were reported in earlier studies.[56]

While colistin treated wild-type cells were morphologically different, the mutated strain *E. coli* NCTC 13846 was on average ~2.5 μm wide and ~150 nm high (Fig. 4G–I), structurally similar to the wild-type *E. coli*. In order to observe colistin interaction with the surface morphology, additional analysis was carried out to measure the root-mean squared roughness denoted by R_q. The R_q was 4.97 ± 1.89 nm, 14.67 ± 4.7 nm and 6.53 ± 1.84 nm for the wild-type *E. coli*, colistin treated *E. coli* as well as *E. coli* NCTC 13846 respectively (Fig. 4J). The roughness was significantly larger for the colistin treated *E. coli* in comparison to the wild-type cells and *E. coli* NCTC 13846. Our results on live *E. coli* cells are similar to the reported roughness values observed on *Acinetobacter baumannii*,[57] where the authors reported an increase in the surface roughness as a function of colistin concentration. Increased roughness is a consequence observed due to the direct interaction of sub-MIC colistin on the cell membrane causing membrane disorder and rearrangement which is the major cause for enhanced lipid diffusion coefficients. Correlating the enhanced dynamics measured using FCS and the modified membrane roughness observed from AFM images, we can establish the effect of sub-MIC concentration of colistin on live bacterial membranes.

4 Conclusions

In this work, we have systematically investigated the changes in lipid diffusion in live bacterial cell membranes exposed to sub inhibitory concentration of colistin. Upon treating the *E. coli* K12 bacterial cells with 0.25 MIC colistin for two hours, we observed elongated cells with a factor of two increase in the lipid diffusion coefficients. It is imperative to note that lipid dynamics observed from inner membrane preferring FM4–64 dye indicated the altered lipid properties in both inner as well

as outer membrane of the *E. coli*. Studying the systematic partitioning of the diffusion coefficients across the bacterial lengths in each system and across the different systems, suggests that the extent of elongation is uncorrelated with the changes observed in the lipid dynamics.

We were able to eliminate the possibility of correlation between growth kinetics, cell elongation and lipid dynamics, which left us with two other possibilities to explain the observed changes in lipid diffusion. The change in diffusivities could be attributed to an outcome of direct interaction between antibiotic molecules on the membrane or an indirect consequence of disruptions in lipid biosynthetic pathways. During the elongation process, it might be possible that the lipid composition is also modulated resulting in the observed increase in diffusivities. Our results from colistin treated *E. coli* NCTC 13846 helps reveal that the altered lipid dynamics observed is due to direct interaction of the colistin molecules on the live inner and outer cell membranes. Finally, we conclude that the dynamics of both inner and outer membrane lipids plays a significant role in the action of a membrane targeting antibiotic at sub-MIC concentrations.

Author contributions

I. I. P., J. S. performed the experiments and analyzed the data. I. I. P., J. S., J. K. B. wrote the paper.

Conflicts of interest

There are no conflicts to declare.

Acknowledgements

The authors thank Prof. K. Ganapathy Ayappa for his constructive guidance during the experiments and Prof. Sandhya Visweswaraiah for her feedback. The authors thank the financial support from the Indian Institute of Science, (IISc), Bengaluru, through the Ministry of Human Resources Development (MHRD)-funded Institute of Eminence (IOE) project.

Notes and references

1 A. J. Ramalingam, *Res. J. Pharm. Technol.*, 2015, **8**, 1719–1724.
2 R. M. Epand, C. Walker, R. F. Epand and N. A. Magarvey, *Biochim. Biophys. Acta, Biomembr.*, 2016, **1858**, 980–987.
3 G. Kapoor, S. Saigal and A. Elongavan, *J. Anaesthesiol., Clin. Pharmacol.*, 2017, **33**, 300.
4 J. G. Hurdle, A. J. O'neill, I. Chopra and R. E. Lee, *Nat. Rev. Microbiol.*, 2011, **9**, 62–75.
5 K. Lohner, *Gen. Physiol. Biophys.*, 2009, **28**, 105–116.
6 S. D. Manning, *Escherichia coli infections*, Infobase Publishing, 2010.
7 J. B. Kaper, J. P. Nataro and H. L. Mobley, *Nat. Rev. Microbiol.*, 2004, **2**, 123–140.
8 M. Mor-Mur and J. Yuste, *Food Bioprocess Technol.*, 2010, **3**, 24–35.
9 M. M. Rahman, A. Husna, H. A. Elshabrawy, J. Alam, N. Y. Runa, A. Badruzzaman, N. A. Banu, M. Al Mamun, B. Paul, S. Das, *et al.*, *Sci. Rep.*, 2020, **10**, 1–11.
10 G. Gregova and V. Kmet, *Sci. Rep.*, 2020, **10**, 1–7.
11 J. Li, S. Xie, S. Ahmed, F. Wang, Y. Gu, C. Zhang, X. Chai, Y. Wu, J. Cai and G. Cheng, *Front. Pharmacol.*, 2017, **8**, 364.
12 M. H. Sharaf, G. M. El-Sherbiny, S. A. Moghannem, M. Abdelmonem, I. A. Elsehemy, A. M. Metwaly and M. H. Kalaba, *Sci. Rep.*, 2021, **11**, 1–16.
13 M. J. Vjecha, S. Tiberi and A. Zumla, *Nat. Rev. Drug Discovery*, 2018, **17**, 607–608.
14 L. M. Lim, N. Ly, D. Anderson, J. C. Yang, L. Macander, A. Jarkowski III, A. Forrest, J. B. Bulitta and B. T. Tsuji, *Pharmacotherapy*, 2010, **30**, 1279–1291.
15 A. B. Janssen and W. van Schaik, *PLoS Genet.*, 2021, **17**, e1009262.
16 E. V. Kift, G. Maartens and C. Bamford, *S. Afr. Med. J.*, 2014, **104**, 183–186.
17 N. K. Khadka, C. M. Aryal and J. Pan, *ACS Omega*, 2018, **3**, 17828–17834.
18 C. Colome, M. Alsina, M. Busquets, I. Haro and F. Reig, *Int. J. Pharm.*, 1993, **90**, 59–71.
19 K. Naghmouchi, J. Baah, D. Hober, E. Jouy, C. Rubrecht, F. Sané and D. Drider, *Antimicrob. Agents Chemother.*, 2013, **57**, 2719–2725.
20 C. Mestres, M. Alsina, M. Busquets, I. Muranyi and F. Reig, *Int. J. Pharm.*, 1998, **160**, 99–107.
21 O. Freudenthal, F. Quilès, G. Francius, K. Wojszko, M. Gorczyca, B. Korchowiec and E. Rogalska, *Biochim. Biophys. Acta, Biomembr.*, 2016, **1858**, 2592–2602.
22 P. Sharma, S. Parthasarathi, N. Patil, M. Waskar, J. S. Raut, M. Puranik, K. G. Ayappa and J. K. Basu, *Langmuir*, 2020, **36**, 8800–8814.
23 D. Z. Rudner, Q. Pan and R. M. Losick, *Proc. Natl. Acad. Sci. U. S. A.*, 2002, **99**, 8701–8706.
24 J. Deich, E. Judd, H. McAdams and W. Moerner, *Proc. Natl. Acad. Sci. U. S. A.*, 2004, **101**, 15921–15926.
25 D. Chow, L. Guo, F. Gai and M. Goulian, *PLoS One*, 2012, **7**, e48600.
26 K. Ritchie and J. Spector, *Biopolymers*, 2007, **87**, 95–101.
27 N. K. Sarangi, K. Ayappa and J. K. Basu, *Sci. Rep.*, 2017, **7**, 1–12.
28 N. K. Sarangi, C. Roobala and J. K. Basu, *Methods*, 2018, **140**, 198–211.
29 N. K. Sarangi, K. Ayappa, S. S. Visweswariah and J. K. Basu, *Langmuir*, 2016, **32**, 9649–9657.
30 N. K. Sarangi, K. Ayappa, S. S. Visweswariah and J. K. Basu, *Phys. Chem. Chem. Phys.*, 2016, **18**, 29935–29945.
31 N. K. Sarangi and J. K. Basu, *Phys. Chem. Chem. Phys.*, 2018, **20**, 29116–29130.

32 C. Roobala and J. K. Basu, *Soft Matter*, 2017, **13**, 4598–4606.
33 R. Chelladurai, K. Debnath, N. R. Jana and J. K. Basu, *Langmuir*, 2018, **34**, 1691–1699.
34 D. I. Andersson and D. Hughes, *Nat. Rev. Microbiol.*, 2014, **12**, 465–478.
35 Y. Sato, Y. Unno, T. Ubagai and Y. Ono, *PLoS One*, 2018, **13**, e0194556.
36 M. E. Wand, L. J. Bock, L. C. Bonney and J. M. Sutton, *J. Antimicrob. Chemother.*, 2015, **70**, 2209–2216.
37 N. R. Council, *et al.*, *Size Limits of Very Small Microorganisms: Proceedings of a Workshop*, 1999.
38 G. Singh, A. C. Chamberlin, H. R. Zhekova, S. Y. Noskov and D. P. Tieleman, *J. Chem. Theory Comput.*, 2016, **12**, 364–371.
39 I. I. Ponmalar, R. Cheerla, K. G. Ayappa and J. K. Basu, *Proc. Natl. Acad. Sci. U. S. A.*, 2019, **116**, 12839–12844.
40 F. Heinemann, V. Betaneli, F. A. Thomas and P. Schwille, *Langmuir*, 2012, **28**, 13395–13404.
41 I. I. Ponmalar, K. G. Ayappa and J. K. Basu, *Biophys. J.*, 2021, **120**, 3040–3049.
42 D. Scherfeld, N. Kahya and P. Schwille, *Biophys. J.*, 2003, **85**, 3758–3768.
43 C. Eggeling, C. Ringemann, R. Medda, G. Schwarzmann, K. Sandhoff, S. Polyakova, V. N. Belov, B. Hein, C. Von Middendorff, A. Schönle, *et al.*, *Nature*, 2009, **457**, 1159–1162.
44 A. Jayol, P. Nordmann, C. André, V. Dubois and L. Poirel, *Int. J. Antimicrob. Agents*, 2017, **50**, 503–504.
45 X. Li and A. W. Smith, *J. Phys. Chem. B*, 2019, **123**, 10433–10440.
46 L. Fu, M. Wan, S. Zhang, L. Gao and W. Fang, *Biophys. J.*, 2020, **118**, 138–150.
47 G. Lindblom and G. Orädd, *Biochim. Biophys. Acta, Biomembr.*, 2009, **1788**, 234–244.
48 E. Falck, M. Patra, M. Karttunen, M. T. Hyvönen and I. Vattulainen, *Biophys. J.*, 2004, **87**, 1076–1091.
49 P. Hinchliffe, Q. E. Yang, E. Portal, T. Young, H. Li, C. L. Tooke, M. J. Carvalho, N. G. Paterson, J. Brem, P. R. Niumsup, *et al.*, *Sci. Rep.*, 2017, **7**, 1–10.
50 I. Fishov and C. L. Woldringh, *Mol. Microbiol.*, 1999, **32**, 1166–1172.
51 A. S. Ghosh and K. D. Young, *J. Bacteriol.*, 2005, **187**, 1913–1922.
52 R. J. Watts, D. Washington, J. Howsawkeng, F. J. Loge and A. L. Teel, *Adv. Environ. Res.*, 2003, **7**, 961–968.
53 F. A. Gogry, M. T. Siddiqui, I. Sultan, F. M. Husain, A. A. AlKheraif, A. Ali, Q. M. Haq, *et al.*, *Pharmaceutics*, 2022, **14**, 295.
54 A. Sabnis, K. L. Hagart, A. Klöckner, M. Becce, L. E. Evans, R. C. D. Furniss, D. A. Mavridou, R. Murphy, M. M. Stevens, J. C. Davies, *et al.*, *eLife*, 2021, **10**, e65836.
55 G. Boix-Lemonche, M. Lekka and B. Skerlavaj, *Antibiotics*, 2020, **9**, 92.
56 A. Bolshakova, O. Kiselyova, A. Filonov, O. Y. Frolova, Y. L. Lyubchenko and I. Yaminsky, *Ultramicroscopy*, 2001, **86**, 121–128.
57 R. L. Soon, R. L. Nation, S. Cockram, J. H. Moffatt, M. Harper, B. Adler, J. D. Boyce, I. Larson and J. Li, *J. Antimicrob. Chemother.*, 2011, **66**, 126–133.